

Limits on Q-ball size due to gravity

TUOMAS MULTAMÄKI*

and

IIRO VILJA†

Department of Physics, University of Turku, FIN-20014, FINLAND

May 28, 2002

Abstract

Solitonic scalar field configurations are studied in a theory coupled to gravity. It is found that non-topological solitons, Q-balls, are present in the theory. Properties of gravitationally self coupled Q-balls are studied by analytical and numerical means. Analytical arguments show that, unlike in the typical flat space scenario, the size of Q-balls is ultimately limited by gravitational effects. Even though the largest Q-balls are very dense, their radii are still much larger than the corresponding Schwarzschild radii. Gravity can also act as a stabilising mechanism for otherwise energetically unstable Q-balls.

*email: tuomul@utu.fi

†email: vilja@utu.fi

1 Introduction

Various field theories can support stable non-topological solitons [1], Q-balls [2], which are coherent scalar condensates that carry a conserved charge, typically a $U(1)$ charge. Due to charge conservation, the Q-ball configuration is the ground state in the sector of fixed charge. Q-balls may have physical importance because the supersymmetric extensions of the Standard Model have scalar potentials that are suitable for Q-balls to exist in the theory. In particular, lepton or baryon number carrying Q-balls are present in the Minimal Supersymmetric Standard Model (MSSM) due to the existence of flat directions in the scalar sector of the theory [3, 4, 5, 6].

Q-balls can be cosmologically significant in various ways. Stable (or long living) Q-balls are natural candidates for dark matter [4] and their decay offers a way to understand the baryon to dark matter ratio [5] as well as the baryon asymmetry of the universe [5, 6]. Q-balls can also protect the baryons from electroweak sphalerons [6] and may be an important factor in considering the stability of neutron stars [7].

For Q-balls to be cosmologically significant, one needs to have a mechanism that creates them in the early stages of the evolution of the universe. Q-balls can be efficiently created in the early universe from an Affleck-Dine (AD) condensate [4, 5]. This process has been studied by numerical simulations [8]-[11] where both the gauge- and gravity-mediated SUSY breaking scenarios were considered. In both cases, Q-balls with various charges have been seen to form from the condensate. Also collisions of Q-balls have been considered in various potentials [9, 12].

A large Q-ball is a very dense object and hence its coupling to the gravitational field may be remarkable. In the present paper we study these aspects of Q-ball solutions *i.e.* we are interested in the gravitational coupling of scalar configurations. Some such considerations have also been studied with reference to Q-stars [13].

The present paper is organised as follows: In Chapter 2 we briefly review the properties of Q-balls in flat space and study analytically the gravitationally coupled system. In Chapter 3 special attention is given to gravitationally coupled thin-walled Q-ball configurations. Numerical results are presented in Chapter 4. The paper is concluded in Chapter 5.

2 Theoretical considerations

2.1 Preliminaries: Q-balls in flat space

Consider a field theory with a $U(1)$ symmetric scalar potential, $V(|\phi|)$, with a global minimum at $\phi = 0$. The complex scalar field ϕ carries a unit quantum number with respect to the $U(1)$ -symmetry. The charge and energy of a field configuration ϕ in D dimensions are [1]

$$Q = \frac{1}{i} \int (\phi^* \dot{\phi} - \dot{\phi} \phi^*) d^D x \quad (1)$$

and

$$E = \int [|\dot{\phi}|^2 + |\nabla\phi|^2 + V(\phi^* \phi)] d^D x. \quad (2)$$

The Q-ball solution is the minimum energy configuration in the sector of fixed charge. A Q-ball is stable against radiative decays into ϕ -scalars if condition

$$E < mQ, \quad (3)$$

where m is the mass of the ϕ -scalar, holds. It is then energetically favourable to store charge in a Q-ball rather than in the form of free scalars.

Finding the minimum energy is straightforward and the Q-ball solution can be shown to be of the form [1, 2]

$$\phi(x, t) = e^{i\omega t} \varphi(r), \quad (4)$$

where $\varphi(x)$ is now time independent and real, ω is the Q-ball frequency (for most cases $|\omega| \in [0, m]$). The charge of a Q-ball with spherical symmetry in D-dimensions is given by

$$Q = 2\omega \int \phi(r)^2 d^D r \quad (5)$$

and the equation of motion at a fixed ω is

$$\frac{d^2\phi}{dr^2} + \frac{D-1}{r} \frac{d\phi}{dr} = \phi \frac{\partial U(\phi^2)}{\partial \phi^2} - \omega^2 \phi. \quad (6)$$

To find the Q-ball solution we must solve (6) with the boundary conditions $\phi'(0) = 0$, $\phi(\infty) = 0$.

The solution of Eq. (6) depends crucially on the shape of the potential. Flat potentials, which are essentially constant over wide range of field φ give rise to the relation $E \propto Q^{3/4}$ [14], whereas in a wide class of more general potentials the energy-charge relations is linear, $E \propto Q$ [1, 2]. However, any Q-ball solution in a potential which is bounded from below, asymptotically increases faster than φ^2 and has a global minimum at the origin, approaches the thin-wall limit when ω becomes small enough. At the thin-wall limit any potential then leads to the linear relation between energy and charge.

2.2 Field equations for gravitationally coupled Q-ball

Supposing that the space time has a maximally symmetric subspace S^2 , *i.e.* the configuration is spherically symmetric, the metric tensor can be written in the form

$$g_{\mu\nu} = \text{diag}(B, -A, -r^2, -r^2 \sin^2 \theta), \quad (7)$$

where A and B are positive functions of time and radial coordinate [15]. A complex scalar field ϕ coupled to gravity is then described by the action

$$S[\phi, A, B] = -\frac{1}{16\pi G} \int d^4x \sqrt{AB} \mathcal{R} + \int d^4x \sqrt{AB} \left(\partial_\mu \phi^\dagger \partial^\mu \phi - V(\phi^\dagger \phi) \right), \quad (8)$$

where \mathcal{R} is the Ricci curvature scalar, $V(\phi^\dagger \phi)$ is the scalar potential and $G = 1/M_{Pl}^2$. By varying the action one obtains the well known Einstein equations together with the equation of motion for the scalar field. They read for the spherically symmetric system in the contracted form as

$$\begin{aligned} -\frac{B''}{2A} + \frac{B'}{4A} \left(\frac{A'}{A} + \frac{B'}{A} \right) - \frac{B'}{Ar} + \frac{\ddot{A}}{2A} - \frac{\dot{A}}{4A} \left(\frac{\dot{A}}{A} + \frac{\dot{B}}{A} \right) &= -4\pi G(\rho + 3P)B, \\ \frac{B''}{2B} - \frac{B'}{4B} \left(\frac{A'}{A} + \frac{B'}{A} \right) - \frac{A'}{Ar} - \frac{\ddot{A}}{2B} + \frac{\dot{A}}{4B} \left(\frac{\dot{A}}{A} + \frac{\dot{B}}{A} \right) &= -4\pi G(\rho - P)A, \\ -1 + \frac{1}{A} - \frac{r}{2A} \left(\frac{A'}{A} - \frac{B'}{B} \right) &= -4\pi G(\rho - P)r^2, \\ -\frac{\dot{A}}{rA} &= -4\pi G \left(\dot{\phi}^\dagger \phi' + \phi'^\dagger \dot{\phi} \right), \\ \phi'' + \phi' \frac{1}{r^2} \sqrt{\frac{A}{B}} \frac{\partial}{\partial r} \left(r^2 \sqrt{\frac{B}{A}} \right) - A \frac{\partial V}{\partial \phi^\dagger} &= \frac{A}{B} \left(\ddot{\phi} + \dot{\phi} \sqrt{\frac{B}{A}} \frac{\partial}{\partial t} \sqrt{\frac{A}{B}} \right), \end{aligned} \quad (9)$$

where the energy density ρ and pressure P are given by

$$\begin{aligned} \rho &= \frac{1}{B} |\dot{\phi}|^2 + \frac{1}{A} |\phi'|^2 + V, \\ P &= \frac{1}{B} |\dot{\phi}|^2 + \frac{1}{A} |\phi'|^2 - V. \end{aligned} \quad (10)$$

The total energy E_{tot} of the Q-ball, including the gravitational energy, is still given by the formula

$$E_{\text{tot}} = \int d^3x \rho, \quad (11)$$

whereas the energy of the scalar configuration without the gravitational contribution, E_s , can be defined as

$$E_s = \int d^3x \sqrt{AB} \rho. \quad (12)$$

Of course, E_{tot} is the true energy of the configuration, but E_s is comparable to the corresponding flat space configuration, as will be shown. In the presence of gravity also the formula for the charge of the Q-ball is modified and is now given by

$$Q = -i\omega \int d^3x \sqrt{AB} (\phi^\dagger \dot{\phi} - \dot{\phi}^\dagger \phi), \quad (13)$$

which differs from the flat space formula by the measure factor \sqrt{AB} .

From the set of equations (9) one can see that the *Ansatz* (4) for the scalar field is still applicable. The right hand side of the equation for R_{tr} then vanishes, implying that A is independent on time. Then, as usual, we can without a loss of generality assume that also B is time independent. The new set of equations now reads as

$$\begin{aligned} -\frac{B''}{2A} + \frac{B'}{4A} \left(\frac{A'}{A} + \frac{B'}{A} \right) - \frac{B'}{Ar} &= -4\pi G(\rho + 3P)B, \\ \frac{B''}{2B} - \frac{B'}{4B} \left(\frac{A'}{A} + \frac{B'}{A} \right) - \frac{A'}{Ar} &= -4\pi G(\rho - P)A, \\ -1 + \frac{1}{A} - \frac{r}{2A} \left(\frac{A'}{A} - \frac{B'}{B} \right) &= -4\pi G(\rho - P)r^2 \end{aligned} \quad (14)$$

and

$$\varphi'' + \varphi' \frac{1}{r^2} \sqrt{\frac{A}{B}} \frac{\partial}{\partial r} \left(r^2 \sqrt{\frac{B}{A}} \right) - AV'_\omega(B, \varphi) = 0. \quad (15)$$

The ω -dependent potential V_ω is defined as

$$V_\omega(B, \varphi) = \frac{1}{2}V(\varphi^2) - \frac{1}{2} \frac{\omega^2}{B} \varphi^2 \quad (16)$$

and V'_ω denotes a derivate of the potential with respect the field φ . The charge of a Q-ball is now given by

$$Q = 8\pi\omega \int_0^\infty dr r^2 \sqrt{A(r)B(r)} \varphi^2. \quad (17)$$

Like in the flat case, a necessary but not a sufficient condition for the existence of Q-balls is that the ω -dependent potential has a non-zero minimum φ_+ with $V_\omega(B, \varphi_+) < V_\omega(B, 0)$ ¹. As usual, this restricts the values of ω , but it also constrains the function B , because V_ω depends explicitly on it. The allowed values for ω are hence restricted to be larger than a critical, non-negative value of ω_c , *i.e.* $\omega > \omega_c$. The critical value, ω_c , is determined by the set of equations

$$\begin{aligned} V_{\omega_c}(1, \varphi_c) &= 0, \\ V'_{\omega_c}(1, \varphi_c) &= 0. \end{aligned} \quad (18)$$

The equations for A and B (14) can be easily solved in terms of ρ and P :

$$\left(\frac{r}{A} \right)' = 1 - 8\pi G r^2 \rho, \quad (19)$$

¹From now on we suppose, that $V_\omega(0) = 0$. We can also choose, without a loss of generality, the central values of A and B to be $A(0) = B(0) = 1$. In addition, for finite energy field configurations $A(\infty) = 1$.

$$\frac{B'}{B} + \frac{A'}{A} = 8\pi G A r (\rho + P). \quad (20)$$

These equations can not, however, be integrated straightforwardly because both ρ and P are dependent on A , B and the field φ . Therefore our aim in the following sections is twofold: In the next section we study the equations and their solutions by utilising analytical approximations in order to gain an understanding of their fundamental properties. To verify these results, Eqs. (14) are studied numerically in Section 4.

3 The thin-wall limit and gravity

If the ω -dependent potential V_ω is such that it fulfils the conventional thin-wall requirements, *i.e.* the height of the barrier is much larger than the difference between minima, the field forms a bubble of radius R . Inside the bubble the value of the field is essentially constant and outside virtually zero with only a thin transition region separating them. The metric components A and B are, however, not constants, but monotonic functions inside the bubble. Thus, one has to determine their behaviour directly from Eqs. (19) and (20). To determine the properties of such a configuration, it is useful to consider the effective action

$$S_\omega = 4\pi \int_0^\infty dr r^2 \sqrt{A(r)B(r)} \left(\frac{1}{2A(r)} \varphi'(r)^2 + V_\omega(B(r), \varphi(r)) \right), \quad (21)$$

from which the equation of motion for φ , Eq. (15), emerges. Applying the usual thin-wall approach to the action (21), leads to some complications due to the presence of gravity. From Eq. (18) we see that two separate sub-cases need to be considered, depending on whether the potential V is monotonic or it has a non-zero local minimum. Defining φ_+ by

$$V'_{\omega_c}(1, \varphi_+) = 0, \quad V''_{\omega_c}(1, \varphi_+) < 0, \quad (22)$$

i.e. φ_+ determines the location of barrier maximum, we can now make a difference between type I and type II thin-wall Q-balls. A thin-wall solution is classified as type I if $V_{\omega_c}(1, \varphi_+) \simeq \omega_c^2 \varphi_c^2$ and type II if $V_{\omega_c}(1, \varphi_+) \gg \omega_c^2 \varphi_c^2$, where φ_c is determined by Eqs. (18). Type I thin-wall hence corresponds to a monotonically increasing potential V whereas type II thin-wall solutions appear when the potential has a non-zero local minimum such that it is nearly degenerate with minimum at $\varphi = 0$.

In both cases we assume that inside the bubble φ is essentially constant. Its value φ_ω is determined by equation

$$V'_\omega(B(R), \varphi_\omega) = 0. \quad (23)$$

Note that even though $B(r)$ is varying inside the bubble, the change is relatively small which justifies our approximation, $B(r) \approx B(R)$.

The value of S_ω inside the bubble is hence given by

$$S_{\omega, in} = 4\pi \int_0^R dr r^2 \sqrt{AB} V_\omega(B(r), \varphi(r)). \quad (24)$$

Note, that now $\omega > \omega_c$ and thus $V_\omega(B(r), \varphi(r)) < 0$ and $E_{\omega, in}$ is negative. Note also that due to Eq. (23), φ_ω depends on the bubble radius R . This negative contribution to E_ω should be balanced by the surface term. If $A(R)$ and $B(R)$ differ only little from unity, the wall contribution can be approximated by

$$S_{\omega, wall} \simeq 4\pi \sigma R^2, \quad (25)$$

where the surface tension is determined by varying the action with the degenerated potential V_ω . In practice this means that, as a first approximation, we set $\omega = \omega_c$, $B = A = 1$, and we finally end up with the usual formula for the surface tension:

$$\sigma \simeq \int_0^{\varphi_c} \sqrt{2V_{\omega_c}(1, \varphi)} d\varphi. \quad (26)$$

Therefore the effective action, reads out as

$$S_\omega = S_{\omega, in} + S_{\omega, wall}. \quad (27)$$

The difference between Eq. (27) and the usual thin-wall case lies in the explicit dependence of Eq. (27) on the metric components A and B . The next step is then to solve A and B from Eqs. (19) and (20). Note, that in this approximation the energy density

$$\rho = \frac{\omega^2}{B}|\varphi|^2 + \frac{1}{A}|\varphi'|^2 + V(\varphi^2) \quad (28)$$

is virtually constant inside the bubble, where one can also neglect the derivative term.

From this point on the two bubble types corresponding to the different types of thin-wall potentials differ from each other and are discussed separately.

3.1 Type I thin-wall solution

For the type I solution the terms $\frac{\omega^2}{B}|\varphi|^2$ and $V(\varphi^2)$ are essentially equal. The relative variation of ρ is also small and hence it is essentially constant. We can thus integrate A out from Eq. (19) and obtain

$$A(r) = \frac{1}{1 - \frac{8\pi}{3}G\rho r^2} = \frac{1}{1 - \frac{16\pi}{3}GV(\varphi_\omega^2)r^2}. \quad (29)$$

Next we note that within the same approximation $\rho + P = \frac{2\omega^2}{B}|\varphi|^2 + \frac{2}{A}|\varphi'|^2 \simeq \frac{2\omega^2}{B}|\varphi|^2$ and Eq. (20) can be rewritten as

$$B' + \frac{A'}{A}B = 16\pi G\omega^2\varphi^2 Ar, \quad (30)$$

which can be solved in the the leading order of G ,

$$B(r) = 1 + \frac{8\pi}{3}GV(\varphi_\omega^2)r^2. \quad (31)$$

We are now able to write down the equations determining the gravitationally coupled thin-wall solution for the Q-balls. We use the solution given above for $B(r)$, solve the relation between R and φ_ω using (23) and calculate R from $\frac{dE_\omega}{dR} = 0$. So, in addition to Eqs. (29) and (31), we have equations

$$V'_\omega(B(R), \varphi_\omega) = 0, \quad 4\pi R^2 \sqrt{A(R)B(R)} V_\omega(B(R), \varphi_\omega) + 8\pi\sigma R = 0, \quad (32)$$

which determine the value of ω as well as R and the corresponding value of the field, φ_ω . Using these values for ω , R and φ_ω we may also calculate the corresponding charge Q from Eq. (17). If A and B do not differ too much from unity we simply obtain

$$Q = \frac{8\pi}{3}\omega\varphi_\omega^2 R^3, \quad (33)$$

where we have neglected the contribution from the wall.

The new features of the gravitationally coupled Q-balls arise due to the non-trivial dependence of the energy inside the bubble to the bubble radius R . Suppose that ω is close enough ω_c . The scale factor $B(R)$ is a monotonically increasing function, and it may happen that at some point the effective ω -parameter $\omega(R) = \omega/\sqrt{B(R)}$ becomes too small and the Eqs. (32) cannot be satisfied. Because R and φ_ω depend implicitly on ω , we are now able to define another critical value of ω , ω_G , as the smallest value where a solution of Eqs. (32) can be found. Thus when gravity effects are taken into account, Q-balls seem to exist only if $\omega > \omega_G$ which, on the other hand, implies maximal a radius R_{max} and maximal charge $Q_{max} = \frac{8\pi}{3}\omega_G\varphi_{\omega_G}^2 R_{max}^3$. The only other possibility is, that the singular point of $A(R)$ is hit first. That, however, would mean that

such a configuration would collapse and form a black hole and hence such Q-balls are not possible either. Clearly, the critical values ω_{\min} , R_{max} and Q_{max} depend explicitly on the shape of the potential and to proceed further one has to define it more precisely.

To see explicitly how the Q-ball charge is constrained, we study a simple example potential. The model potential, V , is constant, m^4 , for $\varphi < \varphi_1$, except near the origin where it tends to zero as φ^2 . The exact behaviour near the origin is not important in our analysis. For values $\varphi > \varphi_1$ the potential increases rapidly, *e.g.* $V \sim \varphi^n$ where the power n is sufficiently large.

Near ω_G , the minimum of V_ω is essentially φ_1 . The metric components are approximately given by

$$\begin{aligned} A(R) &= 1 + \frac{16\pi}{3}GV(\varphi_1^2)R^2 \\ B(R) &= 1 + \frac{8\pi}{3}GV(\varphi_1^2)R^2 \end{aligned}$$

where we have dropped terms higher or equal to $\mathcal{O}(G^2)$. Within the same approximation, we get from Eq. (32) an equation for R :

$$\frac{2\pi Gm^4}{3}R^3(3m^4 - \omega^2\varphi_1^2) + \frac{1}{2}R(m^4 - \omega^2\varphi_1^2) + 2\sigma = 0. \quad (34)$$

Only one of the roots of the cubic equation (34) is physical and is increasing with decreasing ω until the critical point, $\omega = \omega_G$, where the discriminant of the equation vanishes. The maximal value of R is

$$R_{max} = \left(\frac{3\sigma}{2\pi Gm^4(3m^4 - \omega_G^2\varphi_1^2)} \right)^{1/3}. \quad (35)$$

The corresponding charge and energy of the configuration are

$$Q_{max} \approx 2\left(\frac{\varphi_1}{m}\right)^2 \frac{1}{m^2G} \quad (36)$$

$$E_{max} \approx 2\frac{\varphi_1}{m} \frac{1}{mG}, \quad (37)$$

where we have assumed that $\omega_G^2\varphi_1^2 \approx m^4$ and used the approximation $\sigma \sim m^2\varphi_1$. The energy to charge ratio of the maximal Q-ball is $E_{max}/mQ_{max} = m/\varphi_\omega$. In order to see that our approximation is valid, we note that $Gm^4R_{max}^2 \sim (\varphi_1/M_{Pl})^{2/3} \ll 1$.

3.2 Type II thin-wall solution

For the type II solution the fine tuning $V_\omega(B, \phi) \simeq 0$ is not needed in order to reach the thin wall limit because a large barrier exists even without the $\omega^2\phi^2$ -term. Now, indeed, $\omega^2\varphi_\omega^2 \gg V(\varphi_\omega^2)$ and we write an effective energy density as $\rho = (1 + \kappa)\omega^2\varphi^2$, where κ is assumed to be a constant. Instead of equation (29) we now write

$$A(r) = \frac{1}{1 - \frac{8\pi}{3}G\rho r^2} = \frac{1}{1 - \frac{8\pi}{3}G(1 + \kappa)\omega^2\varphi^2 r^2} \quad (38)$$

and from Eq. (30) we obtain by integrating

$$B(r) = 1 + \frac{8\pi}{3}G(2 - \kappa)\omega^2\varphi^2 r^2. \quad (39)$$

The difference between type I and II solutions is that in the type I solution, A increases near the origin twice as fast as B whereas for the type II solution the roles are reversed: B increases roughly twice as fast as A whenever $\kappa \ll 1$.

Due to exactly same reason as before, a minimal ω appears together with a maximal bubble radius, charge and energy in this case as well. Generally, they can again be found solving Eqs. (32), (38) and (39) and searching for the smallest possible ω . However, the procedure is strongly dependent on the explicit form of the potential V as it was in the case of type I solutions.

Therefore, as an example, we again proceed by studying a simple potential

$$V(\varphi^2) = \lambda\varphi^2 \left((\varphi - M)^2 + \epsilon M^2 \right), \quad (40)$$

where M is a mass scale and $\epsilon \ll 1$ is a small positive parameter lifting the non-zero minimum up from $V = 0$. Note, that the quadratic term near the origin reads as $\lambda(1 + \epsilon)M^2\varphi^2$, so that the mass of a single quantum is given by $m^2 \simeq \lambda M^2$. Calculating the surface energy, we find that $\sigma = \sqrt{\lambda}M^3/6$. The set of equations (32) reads now as:

$$\lambda(\varphi_\omega - M)(2\varphi_\omega - M) - \frac{\omega^2}{B(R)} + \omega_c^2 = 0, \quad (41)$$

$$\sqrt{A(R)B(R)} \left(\lambda\varphi_\omega^2(\varphi_\omega - M)^2 + (\omega_c^2 - \frac{\omega^2}{B(R)})\varphi_\omega^2 \right) + \frac{2\sigma}{R} = 0, \quad (42)$$

where $\omega_c^2 = \lambda\epsilon M^2$.

Evidently ω_G is close to ω_c and φ_ω is close to M , which allows us to write $\varphi_\omega = M$ and $\omega = \omega_c$ wherever no explicit difference appears in the formulae. Expanding in the first power of G we arrive at an equation for the bubble radius,

$$R^3 - \frac{3(\omega^2/\omega_c^2 - 1)}{8\pi G\omega_c^2 M^2(2 - \kappa)} R + \frac{3\sigma}{2\pi G\omega_c^4 M^4(2 - \kappa)} = 0. \quad (43)$$

Following the same arguments as in the type I case, we can solve for R_{max} and ω_G :

$$R_{max} = \left(\frac{\sqrt{\lambda}}{4\pi(2 - \kappa)} \frac{M_{Pl}^2}{M\omega_c^4} \right)^{1/3} \quad (44)$$

$$\omega_G^2 = \omega_c^2 \left(1 + 2((2 - \kappa)\pi \frac{M^4}{M_{Pl}^2\omega_c^2})^{1/3} \right). \quad (45)$$

The approximations we made in the process of deriving the above equations constrain the acceptable range of parameter values, $M \ll \sqrt{M_{Pl}\omega_c}$. If this condition is not satisfied our results are not valid and the equations need to be solved numerically.

The maximal charge and energy of a Q-ball in this scenario are

$$Q_{max} \approx \frac{2\sqrt{\lambda}}{3(2 - \kappa)} \frac{MM_{Pl}^2}{\omega_c^3} \quad (46)$$

$$E_{max} \approx \frac{2\sqrt{\lambda}}{3(2 - \kappa)} \frac{MM_{Pl}^2}{\omega_c^2}. \quad (47)$$

The energy to charge ratio, $E_{max}/mQ_{max} = \omega_c/m = \sqrt{\epsilon} \ll 1$, indicates that the maximal Q-ball is energetically stable.

4 Numerical Results

Next we turn to look at some numerical results obtained by computer simulations. We concentrate ourselves to the two different potentials, one with a flat plateau and one with a nearly degenerate minimum. The flat potential allows type I thin wall Q-ball solutions near the critical case. Such potentials are hence called type I potentials. The other type of potential is the one given by

Eq. (40), leading to the type II thin-walls solutions and are therefore called type II potentials. Note, that both of these potential types are represented, *e.g.*, in the MSSM, where the potential arising from gauge mediated supersymmetry breaking is clearly a type I potential whereas gravity mediated supersymmetry breaking typically leads to a type II potential.

From the simulations we have learned, however, that the thin wall limit is exceptionally difficult to study by simulation due to an extreme fine tuning required from the initial value of the field inside the bubble. This fine tuning is much more severe in the gravitationally coupled case, because here one is not attempting to find just the field value, but also a corresponding value of ω . Therefore the simulations are concentrated to the thick-wall end of the parameter space, *i.e.* to larger ω . At best we are able to see some hints of the beginning thin-wall behaviour. Also, in order to clearly demonstrate the observed behaviour of the solutions, we use large mass scales in the potential, since otherwise the true thin-wall solution is needed.

4.1 Type I potential

We begin with a potential

$$V(\varphi^2) = \begin{cases} m^2\varphi^2, & |\varphi| < \varphi_0 \\ m^2\varphi_0^2, & \varphi_0 < |\varphi| < \varphi_1 \\ m^2\varphi_0^2 + \epsilon(\varphi^4 - \varphi_1^4), & \varphi_1 < \varphi \end{cases} \quad (48)$$

where m^2 determines the curvature at the origin, ϵ is a small positive number and $0 < \varphi_0 \ll \varphi_1$. To ensure that the minimum is in the region $\varphi > \varphi_1$ and ω is larger than the critical value, we have to require $m^2 > \omega^2 > 2\epsilon\varphi_1^2$ and $4\epsilon(m^2\varphi_0^2 - \epsilon\varphi_1^4) < \omega^4$, respectively. This potential resembles the flat one discussed in the context of thin-wall configurations. As an example we choose $m = \varphi_0 = 10^{-3}M_{\text{Pl}}$, $\varphi_1^4 = \frac{1}{2}10^{-8}M_{\text{Pl}}^4$, and $\epsilon = 10^{-4}$. For these values, the critical ω equals $\omega_c = \sqrt{2} \times 10^{-1}m$ and the critical field value is just φ_1 . The configuration is studied for several values of ω in order to demonstrate the dependence of the solution on ω . Hence, we take $\omega/m = 0.5, 0.4, 0.3, 0.2$ and 0.142 . In Fig. 1a we have plotted the field configuration of φ and in Fig. 2b the ratio $(B(r) - 1)/(A(r) - 1)$ for these values. Furthermore, in Fig. 2 we have plotted the corresponding energy of the free quanta mQ , total energy E_{tot} and scalar field energy E_s as a function of r for the largest Q-ball corresponding $\omega/m = 0.142$. Note that in Fig. 2, the energy of the free quanta is scaled by a factor of ten, *i.e.* $E_{\text{tot}}, E_s \ll mQ$.

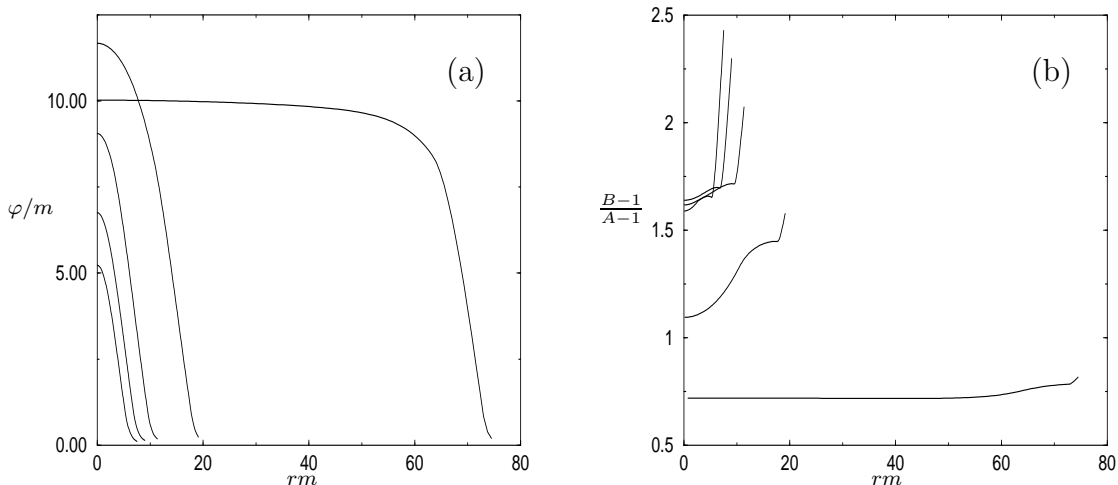


Figure 1: (a) The field profile as function of radial coordinate. (b) The ratio of metric components $(B - 1)/(A - 1)$. In the both figures curves represent values $\omega/m = 0.5$ (the shortest curve), 0.4, 0.3, 0.2 and 0.142 (the longest curve).

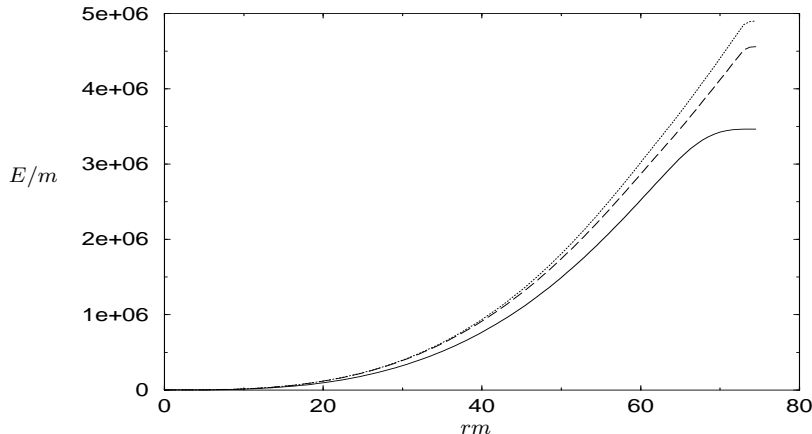


Figure 2: The scaled energy of free quanta $0.1 \times mQ/m$ (solid line), the total energy E_{tot}/m (dashed line) and the scalar field energy E_s/m (dotted line) inside radius rm .

Evidently, for large ω , the profile of φ is thick-walled. However, from the figure it is clear that when ω decreases the configuration tends towards the thin-wall case. This is also reflected by the fact that the ratio $(B(r) - 1)/(A(r) - 1)$ decreases along with decreasing ω . Indeed, according to our analysis of the type I thin-wall configurations, inside the bubble the ratio should approach $\frac{1}{2}$. As can be seen from Fig. 2 the energy difference between E_{tot} and E_s is already for $\omega/m = 0.142$ about 7% and evidently it is increasing with increasing Q-ball size. It should be noted, that the critical ω which is now $\omega_c/m \simeq 0.1414$, is already quite close to the smallest value used in plotting the figure. In the large Q-ball limit, however, the configuration is extremely sensitive to the value of ω .

4.2 Type II potential

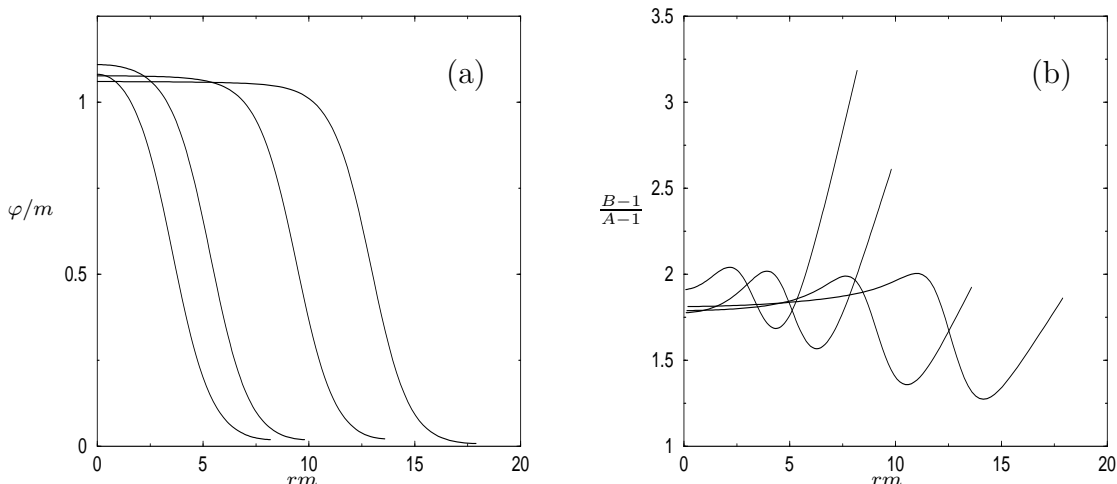


Figure 3: (a) The field profile as function of radial coordinate. (b) The ratio of metric components $(B - 1)/(A - 1)$. In the both figures curves represent values $\omega/m = 0.5, 0.4, 0.3$ and 0.261 .

For numerical studies of potential (40) we choose $\lambda = 1$, $M = 0.0316M_{\text{Pl}}$ and $\epsilon = 10^{-3}$. In Fig. 3a we have plotted the field configuration corresponding to several different values of $\omega/m = 0.5, 0.4, 0.3, 0.261$. The ratio $(B(r) - 1)/(A(r) - 1)$, which inside the bubble equals $(2 - \kappa)/(1 + \kappa)$, is presented in Fig. 3b. Moreover, we now also present in Fig. 4 the energies E_{tot} and E_s as function of the charge Q . For these values of m, λ and ϵ the critical ω is simply given by

$\omega_c^2 = 10^{-3}m^2$. Note, that this time the smallest ω we are able to calculate is $\omega = 0.261 m$ which is significantly bigger than the critical $\omega \simeq 0.0316 m$. This reflects the fact, that the thin-wall type behaviour begins at much larger ratio ω/ω_c for a type II potential than for a type I potential. From Fig. 3b one can also read that the effective parameter κ inside the bubble for small ω is about 0.07. The difference between total and scalar field energies, for the largest plotted balls $Q = 4.8 \times 10^3$, is about 13%.

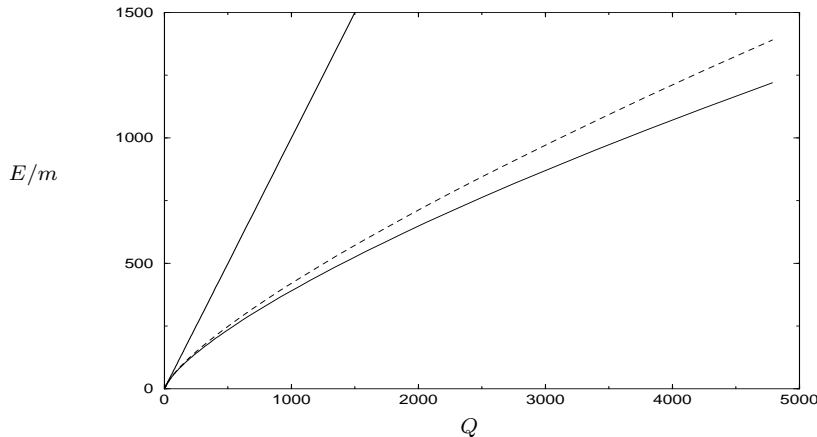


Figure 4: The total energy E_{tot}/m (solid line) and the scalar field energy E_s/m (dotted line) as function of the charge Q . The smallest Q corresponds to $\omega/m = 0.995$ whereas the largest one corresponds to $\omega/m = 0.261$. The straight line is the $E = mQ$ curve.

5 Discussion and Conclusions

In this paper we have considered the effects of gravity on Q-ball type scalar field configurations. Including the effects of gravity leaves the flat space Q-ball *Ansatz* valid; one still has a spherically symmetric solution whose complex phase rotates uniformly with time. The geometry of space-time is modified from the flat case, which gives a contribution to the charge and energy of the configuration.

From the analytical and numerical work it is evident that the effects of gravity can give a large contribution to the Q-ball energy. However, in order for the contribution to be significant, either the free quanta of the Q-ball scalar field need to be extremely heavy or the charge of the Q-ball needs to be very large. The gravitational contribution is strongly dependent on the details of the potential and needs, in general, to be computed numerically.

Interesting points are raised by the analytical analysis. The analytical work is concentrated on the thin-wall limit, in order to gain an understanding of the properties of large Q-balls for which gravitational effects are more likely to be significant. In the thin-wall limit, analytical considerations reveal that the maximal size of Q-balls is ultimately limited by gravity. The non-trivial geometry inside the Q-ball limits the size of Q-balls for any potential that allows for Q-ball solutions. The physical reasoning behind this is simple. In equilibrium, the rotation of the complex phase generates an outward pressure which prevents the Q-ball from collapsing due to gravitational forces. In the ordinary thin-wall limit, the Q-ball frequency tends a critical value ω_c , while the charge the Q-ball becomes larger and larger. If gravity is included in the scenario, it is evident that at some point the Q-ball becomes too large to be balanced by the internal pressure. Hence, there exists another critical value, $\omega_G > \omega_c$, corresponding to the maximally large Q-ball.

The limit on the maximal Q-ball size due to the gravitational effects is an interesting point raised by this analysis. The two example potentials discussed approximately correspond to the

potentials associated with gauge (type I) and gravity (type II) mediated supersymmetry breaking. Using typical values for the variables, $m \sim 100$ GeV, $\varphi_1 \sim M \sim 10^{15}$ GeV, and approximating $\omega_c \sim m$, estimates for the maximum charge, energy and radius are: $Q_{max} \sim 10^{60}$, $E_{max} \sim 10^{49}$ GeV, $R_{max} \sim 10^{13}$ GeV $^{-1} \sim 0.1$ cm (type I) and $Q_{max} \sim 10^{34}$, $E_{max} \sim 10^{36}$ GeV, $R_{max} \sim 1$ GeV $^{-1}$ (type II). In both cases, the Schwarzschild radius of a corresponding black hole is still much smaller than that of the Q-ball. Gravity will clearly not have a very significant role to play in a cosmological setting for Q-balls in the gauge mediated scenario. In the gravity mediated scenario the limit is much lower and may be significant. It is interesting to note that, in order for the primordial Q-balls to act as a self-interacting dark matter candidate [16], one typically has to consider Q-balls with very large charges [17].

Since the gravitational contribution to the Q-ball energy is negative, it is possible that gravity can render an otherwise energetically unstable Q-ball stable. This behaviour was also confirmed by the numerical work, where it was observed that the negative energy of the gravitational field could stabilise a large enough Q-ball. One can then envision a cosmological scenario where Q-balls are unstable, and hence do not exist, unless their charge is large enough for the gravitational effects to stabilise them. A primordial Q-ball distribution formed at a large energy scale would then leave behind only stable, super heavy relic Q-balls.

Acknowledgements

This work has been partly supported by the Magnus Ehrnrooth Foundation.

References

- [1] T. D. Lee and Y. Pang, *Phys. Rev.* **221** (1992) 251.
- [2] S. Coleman, *Nucl. Phys.* **B262** (1985) 263.
- [3] A. Kusenko, *Phys. Lett.* **B405** (1997) 108.
- [4] A. Kusenko and M. Shaposhnikov, *Phys. Lett.* **B418** (1998) 46.
- [5] K. Enqvist and J. McDonald, *Nucl. Phys.* **B538** (1999) 321.
- [6] K. Enqvist and J. McDonald, *Phys. Lett.* **B425** (1998) 309.
- [7] A. Kusenko *et al.*, *Phys. Lett.* **B423** (1998) 104.
- [8] S. Kasuya and M. Kawasaki, *Phys. Rev. D* **61** (2000) 041301.
- [9] S. Kasuya and M. Kawasaki, *Phys. Rev. D* **62** (2000) 023512.
- [10] K. Enqvist, A. Jokinen, T. Multamäki and I. Vilja, *Phys. Rev. D* **63** (2001) 083501.
- [11] T. Multamäki and I. Vilja, hep-ph/0203195, *to appear in Phys. Lett. B*.
- [12] M. Axenides *et al.*, *Phys. Rev. D* **61** (2000) 085006; R. A. Battye and P. M. Sutcliffe, *Nucl. Phys.* **B590** (2000) 329; T. Multamäki and I. Vilja, *Phys. Lett.* **B482** (2000) 161; T. Multamäki and I. Vilja, *Phys. Lett.* **B484** (2000) 283.
- [13] B. W. Lynn, *Nucl. Phys.* **B321** (1989) 465.
- [14] G. Dvali, A. Kusenko and M. Shaposhnikov, *Phys. Lett.* **B417** (1998) 99.
- [15] See *e.g.* S. Weinberg, *Gravitation and Cosmology*, Wiley, 1972.
- [16] A. Kusenko and P. Steinhardt, *Phys. Rev. Lett.* **87** (2001) 141301.
- [17] K. Enqvist *et al.*, *Phys. Lett.* **B526** (2002) 9.